AIAA 80-1527R

# Unsteady Compressible Laminar Boundary-Layer Flow within a Moving Expansion Wave

Lang Mann Chang*
*U.S. Army Ballistic Research Laboratory, Aberdeen Proving Ground, Md.*
and
Ching-Jen Chen†
*The University of Iowa, Iowa City, Iowa*

**Numerical solutions for the unsteady compressible laminar boundary-layer flow developed within a centered expansion wave are obtained for two wall thermal conditions, isothermal and adiabatic. The Howarth's transformation, similarity transformation via one-parameter groups, and then series expansion are employed for the solutions. The solutions are of second-order accuracy and are shown to improve over the Hall's zero-order solution for the temperature distribution in the boundary layer. It is shown that both velocity and temperature boundary layer grow rapidly behind the expansion wavefront but attenuate further downstream. If the wall temperature is held at the undisturbed temperature, the heat transfer occurs from the wall to the expanding gas. The rate of heat transfer increases from the wavefront to approximately $\xi = 0.35$ behind the wave where maximum heat transfer is observed. The isothermal wall temperature is found to be higher than the adiabatic wall temperature by a factor $(1 + 0.335\xi)$.**

## Nomenclature

| | |
|---|---|
| $C_f$ | = coefficient of local skin friction |
| $C_p$ | = specific heat at constant pressure |
| $F$ | = inviscid velocity function, Eq. (1) |
| $F^*$ | = function of $z$, Appendix and Eq. (33) |
| $f$ | = transformed streamfunction, Eq. (21) |
| $f_n$ | = transformed streamfunction, Eq. (26), $n = 1,2,3,...$ |
| $G$ | = inviscid temperature function, Eq. (2) |
| $G^*$ | = function of $z$ set, Appendix and Eq. (34) |
| $g$ | = transformed temperature function, Eq. (22) |
| $g_n$ | = transformed temperature function, Eq. (28) |
| $H$ | = inviscid pressure function, Eq. (3) |
| $h$ | = heat transfer coefficient |
| $k$ | = thermal conductivity |
| $L$ | = reference length |
| $n$ | = integer, $n = 0,1,2,...$ |
| $p$ | = dimensionless pressure |
| $\bar{p}$ | = dimensional pressure |
| $p_i$ | = dimensionless freestream pressure |
| $Pr$ | = Prandtl number |
| $Re$ | = Reynolds number |
| $Q_w$ | = dimensional heat flux at the wall |
| $q_w$ | = dimensionless heat flux at the wall |
| $R$ | = gas constant |
| $T$ | = dimensional temperature |
| $T_i$ | = dimensional freestream temperature |
| $T_0$ | = temperature of the undisturbed fluid |
| $T_r$ | = reference temperature $U_r^2/R = \gamma T_0$ |
| $T_w$ | = wall temperature |
| $t$ | = dimensionless time $\bar{t}U_r/L$ |
| $\bar{t}$ | = dimensional time |
| $t^*$ | = dimensionless time, Fig. 1 |
| $U$ | = $x$-component velocity, dimensional |
| $U_r$ | = reference velocity, speed of the expansion wavefront $\sqrt{\gamma R T_0}$ |
| $u$ | = $x$-component velocity, dimensionless, Eq. (6) |
| $u_i$ | = dimensionless freestream velocity |
| $V$ | = $y$-component velocity, dimensional |
| $v$ | = $y$-component velocity, dimensionless, Eq. (6) |
| $x, y'$ | = dimensionless coordinates, Fig. 1 and Eq. (6) |
| $\bar{x}, Y$ | = dimensional coordinates |
| $y$ | = dimensionless, transformed coordinate $y'$, Eq. (1) |
| $z$ | = variable, Eq. (25) |
| $\gamma$ | = ratio of specific heats |
| $\eta$ | = similarity variable, Eq. (20) |
| $\theta$ | = dimensionless temperature |
| $\theta_i$ | = dimensionless freestream temperature |
| $\theta_w$ | = dimensionless wall temperature |
| $\mu$ | = dimensionless viscosity |
| $\bar{\mu}$ | = dimensional viscosity |
| $\mu_r$ | = reference viscosity |
| $\xi$ | = similarity variable, Eq. (20) |
| $\rho$ | = dimensionless density, Eq. (6) |
| $\bar{\rho}$ | = dimensional density |
| $\rho_r$ | = reference density |
| $\psi$ | = modified streamfunction, Eq. (12) |
| $\infty$ | = outer edge of the boundary layer |

*Subscripts*

| | |
|---|---|
| $i$ | = inviscid |
| $r$ | = reference |
| $w$ | = wall condition |
| 0 | = undisturbed |

Presented as Paper 80-1527 at the AIAA 15th Thermophysics Conference, Snowmass, Colo., July 14-16, 1980; submitted Jan. 13, 1981; revision received May 12, 1981. 

*Research Engineer, Interior Ballistic Division.

†Professor and Senior Research Scientist, Energy Division and Iowa Institute of Hydraulic Research. Member AIAA.

## I. Introduction

THE present paper studies the velocity and temperature boundary-layer development within a centered expansion wave moving into a stationary fluid. A centered expansion wave can be generated either in a shock tube or a tube wind tunnel such as designated by Ludweig.[1] The problem considers that a fluid is initially at the uniform temperature $T_0$ but is separated in two regions, one at a high and the other at a low pressure. If the diaphragm is suddenly removed, an expansion wave is formed and propagates into the stationary high pressure region. In the expansion region the temperature of the fluid will be decreased due to the drop in the pressure. Therefore, if the wall is kept at the initial temperature $T_0$, there will result the net heat transfer from the wall to the fluid in the expansion region. The heat transfer and boundary-layer development in the expansion region is the subject of the present analysis.

As early as 1859 Riemann analyzed the fundamental relationships for the propagation of plane disturbance of finite amplitude in an unsteady one-dimensional isotropic flow.[2] This was followed by many studies on the shock tube problem. Huber et al., for example, provided analytical expressions for the velocity, pressure, and temperature of the inviscid flow.[3] However, in order to calculate the heat transfer characteristics, the boundary-layer development on the inner wall cannot be neglected. Mirels analyzed the boundary-layer flow behind the expansion wave by assuming that the expansion wave is a line of discontinuity separating the undisturbed high pressure region from the rarefied gas region.[4] Subsequently, Cohen used the coordinate expansion method to solve the boundary-layer flow within the centered expansion wave with a finite width.[5] This treatment, which is an improvement over the Mirels' solution, is based on the assumption that the thermal conductivity of the isothermal wall is infinite. Hall later generalized the Cohen solution by allowing the wall to have a finite thermal conductivity.[6] Solutions of heat transfer for some representative values of thermal conductivity are given by Hall. Hall shows that in the case of adiabatic wall the zeroth-order solution for the temperature in the boundary layer has no difference from the temperature in the freestream.

The present study provides further solutions for the boundary-layer flow subject to the two wall thermal conditions, one adiabatic and one held at the isothermal undisturbed fluid temperature. The solutions are obtained by applying Howarth's transformation and the similarity transformation via one-parameter groups which reduces the number of independent variables from three, i.e., a time and two spatial variables, to two. Then the solutions are expanded in a series. The first three terms of the series are solved providing a solution of second-order accuracy.[7-9]

## II. Problem Formulation

The boundary-layer flow in the region of the expansion wave as shown in Fig. 1 is considered to be two dimensional, unsteady, compressible, and laminar. The fluid is an ideal gas. External to the boundary layer, the flow is assumed to be an unsteady one-dimensional inviscid flow. The solution of the inviscid flow is considered known and is used as the matching condition for the boundary-layer solution.

If the undisturbed region is kept at a temperature $T_0$ it is known that the wavefront of the expansion wave propagates at a sound speed of $U_r$ or $(\gamma R T_0)^{1/2}$. The velocity relative to the wavefront, temperature, and pressure distribution in the expansion region outside the boundary layer expressed in terms of the similarity variable $\xi$ are given by Huber et al.[3] as

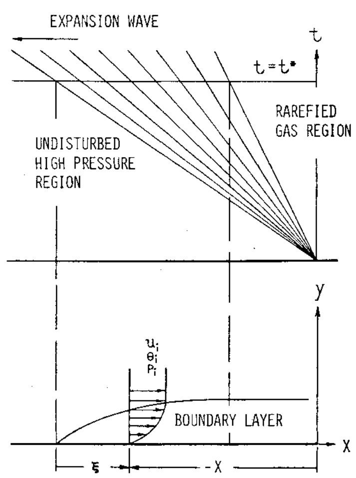


**Fig. 1 Shock tube flow at $t=t^*$.**

Velocity

$$u_i(t,x) = \frac{2}{\gamma+1}\xi = F(\xi) \tag{1}$$

Temperature

$$\theta_i(t,x) = \frac{1}{\gamma}\left(1-\frac{\gamma-1}{\gamma+1}\xi\right)^2 = G(\xi) \tag{2}$$

Pressure

$$p_i(t,x) = \left(1-\frac{\gamma-1}{\gamma+1}\xi\right)^{2\gamma/(\gamma-1)} = H(\xi) \tag{3}$$

where the similarity variable $\xi$, which can be derived from the similarity transformation via one-parameter groups, is

$$\xi = 1+(x/t) \tag{4}$$

As shown in Fig. 1, $\xi=0$ denotes the expansion wavefront and $\xi=1$ is located at the origin of the wave. $F(\xi)$, $G(\xi)$, and $H(\xi)$ are, respectively, the velocity function, temperature function, and pressure function of the inviscid flow. The velocity $u_i$ is the inviscid velocity normalized by the speed of the expansion wavefront $U_r$, the temperature $\theta_i$ by the reference temperature $T_r = U_r^2/R$, and the pressure $p_i$ by the product of $P_r = \rho_r U_r^2$. $\rho_r$ is the reference density evaluated at the reference temperature $T_r$ and pressure $P_r$ through the ideal gas equation. $\gamma$ is the ratio of specific heats. In the boundary layer we assume that the thermal conductivity $k$ and specific heat $C_p$ are constants but that the viscosity $\bar{\mu}$ is proportional to the temperature and is made dimensionless by $\mu_r$, or

$$\mu = \bar{\mu}/\mu_r = T/T_r \tag{5}$$

where the reference viscosity $\mu_r$ is evaluated at the reference temperature $T_r$. The following dimensionless variables and parameters are defined for the boundary-layer equation:

$$t=\bar{t}L/U_r, \quad x=X/L, \quad y'=Re^{1/2}Y/L, \quad u=U/U_r$$

$$v=Re^{1/2}V/U_r, \quad p=P/(\rho_r U_r^2), \quad \theta=T/T_r, \quad \rho=\bar{\rho}/\rho_r,$$

$$Re=U_r L\rho_r/\mu_r, \quad Pr=C_p\mu_r/k, \quad T_r=U_r^2/R \tag{6}$$

The governing equations for the two-dimensional, unsteady, compressible boundary-layer flow are

Continuity

$$\frac{\partial\rho}{\partial t}+\frac{\partial}{\partial x}(\rho u)+\frac{\partial}{\partial y'}(\rho v)=0 \tag{7}$$

Momentum

$$\rho\left(\frac{\partial u}{\partial t}+u\frac{\partial u}{\partial x}+v\frac{\partial u}{\partial y'}\right)=-\frac{\mathrm{d}p}{\mathrm{d}x}+\frac{\partial}{\partial y'}\left(\mu\frac{\partial u}{\partial y'}\right) \tag{8}$$

Energy

$$\rho\left(\frac{\partial\theta}{\partial t}+u\frac{\partial\theta}{\partial x}+v\frac{\partial\theta}{\partial y'}\right)=\frac{1}{Pr}\frac{\partial}{\partial y'}\left(\theta\frac{\partial\theta}{\partial y'}\right)$$

$$+\frac{\gamma-1}{\gamma}\left[\frac{\partial p}{\partial t}+u\frac{\partial p}{\partial x}+\theta\left(\frac{\partial u}{\partial y'}\right)^2\right] \tag{9}$$

State

$$p=\rho\theta \tag{10}$$

After introducing Howarth's transformation[7]

$$y=\int_0^{y'} \rho \mathrm{d}y' \tag{11}$$

a streamfunction $\psi$, which satisfies the continuity equation, can be defined as

$$u=\frac{\partial\psi}{\partial y}, \quad v=-\frac{1}{\rho}\left(\frac{\partial\psi}{\partial x}+\frac{\partial\psi}{\partial y}\frac{\partial y}{\partial x}+\frac{\partial y}{\partial t}\right) \tag{12}$$

Substituting Eqs. (11) and (12) into Eqs. (8) and (9), we have

Momentum

$$\frac{\partial^2\psi}{\partial t\partial y}+\frac{\partial\psi}{\partial y}\frac{\partial^2\psi}{\partial x\partial y}-\frac{\partial\psi}{\partial x}\frac{\partial^2\psi}{\partial y^2}=-\frac{\theta}{p}\frac{\mathrm{d}p}{\mathrm{d}x}+p\frac{\partial^3\psi}{\partial y^3} \tag{13}$$

Energy

$$\frac{\partial\theta}{\partial t}+\frac{\partial\psi}{\partial y}\frac{\partial\theta}{\partial x}-\frac{\partial\psi}{\partial x}\frac{\partial\theta}{\partial y}=\frac{p}{Pr}\frac{\partial^2\theta}{\partial y^2}+\frac{\gamma-1}{\gamma}\left(\frac{\theta}{p}\right)$$

$$\times\left[\frac{\partial p}{\partial t}+\frac{\partial\psi}{\partial y}\frac{\partial p}{\partial x}+\frac{p^2}{\theta}\left(\frac{\partial^2\psi}{\partial y^2}\right)^2\right] \tag{14}$$

To solve these two equations for $\psi$ and $\theta$ the following boundary conditions are specified.

At the wall, $y=0$

$$u=\frac{\partial\psi}{\partial y}=0 \quad \text{(no slip condition)} \tag{15}$$

$$v=-\frac{1}{\rho}\frac{\partial\psi}{\partial x}=0 \quad \text{(impermeable condition)}$$

$$\theta=\theta_w=\frac{1}{\gamma} \quad \text{(isothermal wall at } T_0\text{)} \tag{16}$$

$$\frac{\partial\theta}{\partial y}=0 \quad \text{(adiabatic wall)} \tag{17}$$

At the outer edge of the boundary layer, $y\to\infty$

$$u=\frac{\partial\psi}{\partial y}=u_i(t,x) \tag{18}$$

$$\theta=\theta_i(t,x) \tag{19}$$

## III. Method of Solution

The solution is obtained through a similarity transformation via one-parameter groups and then a series expansion. The similarity transformation which allows us to reduce the three independent variables $(t,x,y)$ into two similarity variables $(\xi,\eta)$ are

$$\xi=1+(x/t) \quad \text{and} \quad \eta=y/t^{1/2} \tag{20}$$

The detailed derivation of these two similarity variables is given by Chang.[10] The similarity transformation also transforms the dependent variables, streamfunction, and temperature, into

$$\psi(t,x,y)=t^{1/2}f(\xi,\eta) \tag{21}$$

$$\theta(t,x,y)=g(\xi,\eta) \tag{22}$$

Substitution of Eqs. (3) and (20-22) into Eqs. (13) and (14) results in

Momentum

$$(1-\xi)f_{\xi\eta}-\frac{1}{2}\eta f_{\eta\eta}+f_\eta f_{\xi\eta}-f_\xi f_{\eta\eta}=-g\frac{H'}{H}+Hf_{\eta\eta\eta} \tag{23}$$

Energy

$$(1-\xi)g_\xi-\frac{1}{2}\eta g_\eta+f_\eta g_\xi-f_\xi g_\eta=\frac{1}{Pr}Hg_{\eta\eta}$$

$$+\frac{\gamma-1}{\gamma}\frac{g}{H}\left[(1-\xi)H'+f_\eta H'+\frac{H^2}{g}f_{\eta\eta}^2\right] \tag{24}$$

where $H'$ is the derivative of $H(\xi)$ with respect to $\xi$. A repeated application of the transformation to find new similarity variables that will combine the variables $\xi$ and $\eta$ does not exist. However, the method does help to define a new locally similar variable $z$, which makes the differential

**Table 1 Velocity functions**

| | Isothermal wall | | | Adiabatic wall | | |
|---|---|---|---|---|---|---|
| $z$ | $f_0'$ | $f_1'$ | $f_2'$ | $f_0'$ | $f_1'$ | $f_2'$ |
| 0 | 0.00000 | 0.00000 | 0.00000 | 0.00000 | 0.00000 | 0.00000 |
| 0.2 | 0.20643 | 0.13364 | 0.06425 | 0.20643 | 0.11252 | 0.05276 |
| 0.4 | 0.37735 | 0.22220 | 0.09358 | 0.37735 | 0.18962 | 0.08014 |
| 0.6 | 0.51717 | 0.27376 | 0.09495 | 0.51717 | 0.23642 | 0.08529 |
| 0.8 | 0.63011 | 0.29602 | 0.07631 | 0.63011 | 0.25834 | 0.07322 |
| 1.0 | 0.72016 | 0.29611 | 0.04555 | 0.72016 | 0.26084 | 0.04973 |
| 1.2 | 0.79100 | 0.28046 | 0.00973 | 0.79100 | 0.24907 | 0.02052 |
| 1.4 | 0.84596 | 0.25460 | −0.02540 | 0.84596 | 0.22773 | −0.00945 |
| 1.6 | 0.88801 | 0.22310 | −0.05576 | 0.83800 | 0.20081 | −0.03638 |
| 1.8 | 0.91971 | 0.18957 | −0.07788 | 0.91971 | 0.17156 | −0.05778 |
| 2.0 | 0.94325 | 0.15666 | −0.09373 | 0.94325 | 0.14245 | −0.07243 |
| 2.4 | 0.97288 | 0.09917 | −0.10045 | 0.97288 | 0.09087 | −0.08185 |
| 2.8 | 0.98783 | 0.05719 | −0.08558 | 0.98783 | 0.05271 | −0.07162 |
| 3.0 | 0.99205 | 0.04202 | −0.07417 | 0.99205 | 0.03882 | −0.06261 |
| 3.4 | 0.99680 | 0.02128 | −0.05023 | 0.99680 | 0.01975 | −0.04287 |
| 3.8 | 0.99848 | 0.00989 | −0.03016 | 0.99884 | 0.00925 | −0.02585 |
| 4.0 | 0.99935 | 0.00653 | −0.02246 | 0.99935 | 0.00615 | −0.01924 |
| 5.0 | 1.00010 | 0.00047 | −0.00389 | 1.00010 | 0.00062 | −0.00317 |
| 6.0 | 1.00020 | 0.00018 | −0.00696 | | | |
| 7.0 | 1.00020 | −0.00064 | −0.00110 | | | |
| 8.0 | 1.00020 | −0.00099 | −0.00125 | | | |

**Table 2 Temperature functions**

| | Isothermal wall | | | Adiabatic wall | | |
|---|---|---|---|---|---|---|
| $z$ | $g_0$ | $g_1$ | $g_2$ | $g_0$ | $g_1$ | $g_2$ |
| 0 | 0.00000 | 0.00000 | 0.00000 | 1.00000 | −0.18805 | −0.12156 |
| 0.2 | 0.17756 | 0.03701 | −0.02294 | 1.00000 | −0.17984 | −0.10638 |
| 0.4 | 0.32907 | 0.07981 | −0.01369 | 1.00000 | −0.16077 | −0.07399 |
| 0.6 | 0.45723 | 0.11981 | 0.00384 | 1.00000 | −0.13707 | −0.03825 |
| 0.8 | 0.56468 | 0.15207 | 0.01733 | 1.00000 | −0.11271 | −0.00685 |
| 1.0 | 0.65394 | 0.17434 | 0.02195 | 1.00000 | −0.09000 | 0.01685 |
| 1.2 | 0.72739 | 0.18629 | 0.01737 | 1.00000 | −0.07014 | 0.03229 |
| 1.4 | 0.78705 | 0.18880 | 0.00563 | 1.00000 | −0.05352 | 0.04042 |
| 1.6 | 0.83554 | 0.18346 | −0.01035 | 1.00000 | −0.04009 | 0.04285 |
| 1.8 | 0.87411 | 0.17213 | −0.02768 | 1.00000 | −0.02954 | 0.04134 |
| 2.0 | 0.90460 | 0.15673 | −0.04395 | 1.00000 | −0.02144 | 0.03744 |
| 2.4 | 0.94689 | 0.12032 | −0.06726 | 1.00000 | −0.01084 | 0.02695 |
| 2.8 | 0.97167 | 0.08461 | −0.07489 | 1.00000 | −0.00522 | 0.01717 |
| 3.0 | 0.97969 | 0.06891 | −0.07341 | 1.00000 | −0.00356 | 0.01323 |
| 3.4 | 0.98994 | 0.04334 | −0.06322 | 1.00000 | −0.00159 | 0.00742 |
| 3.8 | 0.99532 | 0.02553 | −0.04868 | 1.00000 | −0.00068 | 0.00389 |
| 4.0 | 0.99691 | 0.01916 | −0.04068 | 1.00000 | −0.00436 | 0.00275 |
| 5.0 | 0.99996 | 0.00383 | −0.01248 | 1.00000 | −0.00002 | 0.00041 |
| 6.0 | 1.00050 | 0.00081 | −0.00270 | | | |
| 7.0 | 1.00060 | 0.00033 | −0.00101 | | | |
| 8.0 | 1.00080 | 0.00007 | −0.00100 | | | |

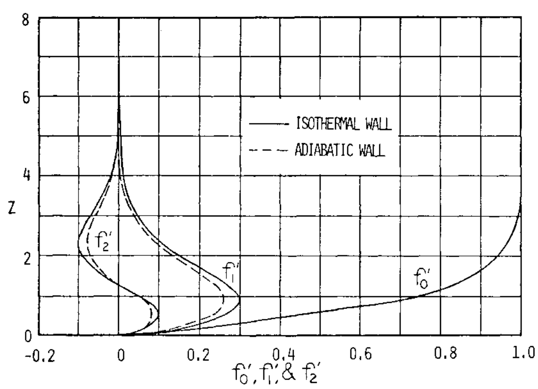


Fig. 2 Profiles of velocity functions.

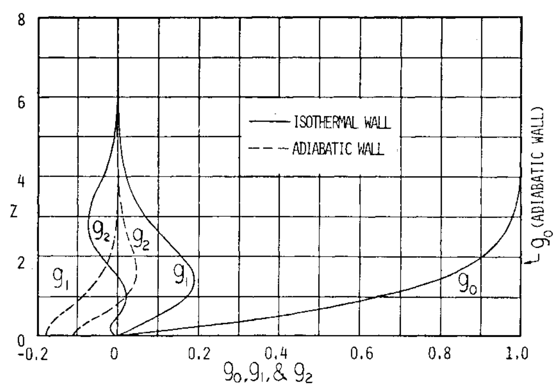


Fig. 3 Profiles of temperature functions.

equations depend the least on the variable $\xi$

$$z=\eta/\xi^{1/2} \tag{25}$$

With the new variable $z$, a fast-convergent series solution to the problem may be constructed.

The series solution for the streamfunction, velocity, and temperature then are sought in the following form:

$$f=\xi^{1/2}F(\xi)=\sum_{n=0}^{\infty}\xi^n f_n(z) \tag{26}$$

$$u=\frac{\partial\psi}{\partial y}=\frac{\partial f}{\partial\eta}=F(\xi)\sum_{n=0}^{\infty}\xi^n f_n'(z) \tag{27}$$

$$\theta=g(\xi,\eta)=\frac{1}{\gamma}+\left[G(\xi)-\frac{1}{\gamma}\right]\sum_{n=0}^{\infty}\xi^n g_n(z) \tag{28}$$

The functions $f_n(z)$ and $g_n(z)$ are functions of $z$ only. Substituting Eqs. (26-28), and their derivatives into Eqs. (23) and (24), we have, after grouping the terms with the same power of $\xi$, the following system of ordinary differential equations.

Zero-order equations ($n=0$)

$$f_0'''+{}^1\!/\!_2 zf_0''-f_0'=-1 \tag{29}$$

$$(1/Pr)g_0''+{}^1\!/\!_2 zg_0'-g_0=-1 \tag{30}$$

First-order equations ($n=1$)

$$f_1'''+\frac{1}{2}zf_1''-2f_1'=\frac{2\gamma}{\gamma+1}f_0'''-\frac{3}{\gamma+1}f_0''f_0-f_0' + \frac{2}{\gamma+1}(f_0')^2+2\frac{\gamma-1}{\gamma+1}g_0-\frac{\gamma-1}{\gamma+1} \tag{31}$$

$$\frac{1}{Pr}g_1''+\frac{1}{2}zg_1'-2g_1=\frac{1}{Pr}\frac{5\gamma-1}{2(\gamma+1)}g_0''+\left(\frac{z}{4}\frac{\gamma-1}{\gamma+1}\right)g_0' - \left(\frac{2}{\gamma+1}\right)g_0-\left(\frac{3}{\gamma+1}\right)g_0'f_0+\left(\frac{2}{\gamma+1}\right)f_0''^2 - \left(\frac{2}{\gamma+1}\right)f_0'+\left(\frac{2}{\gamma+1}\right)f_0'g_0+\frac{2}{\gamma+1} \tag{32}$$

Second-order equations ($n=2$)

$$f_2'''+{}^1\!/\!_2 zf_2''-3f_2'=F^*(z) \tag{33}$$

$$(1/Pr)g_2''+{}^1\!/\!_2 zg_2'-3g_2=G^*(z) \tag{34}$$

The functions $F^*(z)$ and $G^*(z)$ are given in the Appendix. The boundary conditions Eqs. (15-19) become the following.

At the wall, $z=0$, for $n \geq 0$

$$f_n(0)=0, \quad f_n'(0)=0$$

$$g_n(0)=0 \quad \text{for isothermal wall}$$

$$g_n'(0)=0 \quad \text{for adiabatic wall} \tag{35}$$

At the outer edge of the boundary layer, $z \to \infty$

$$f_0'(\infty)=1, \quad f_n'(\infty)=0 \quad \text{for } n \geq 1$$

$$g_0(\infty)=1, \quad g_n(\infty)=0 \quad \text{for } n \geq 1$$

$$g_n'(\infty)=0 \quad \text{for } n \geq 0 \tag{36}$$

## IV. Results and Discussion

The preceding three sets of ordinary differential equations were solved numerically.[10] With $Pr=0.72$ and $\gamma=1.4$ the numerical results of the velocity functions $f_0'$, $f_1'$, and $f_2'$, and the temperature functions $g_0$, $g_1$, and $g_2$ for both isothermal and adiabatic walls are tabulated in Tables 1 and 2 and plotted in Figs. 2 and 3. Since there is no temperature term involved in the zero-order momentum equation Eq. (29), the function $f_0'$ is independent of the temperature condition at the wall. Therefore, as shown in Fig. 2, the velocity function $f_0'$ is the same for the two wall conditions. However, the functions $f_1'$ and $f_2'$ are certainly affected by the wall temperature. For the case of isothermal wall the present results are identical to Cohen's solutions.[10]

With the zero-order, first-order, and second-order functions computed, the solutions to the problem in a three-term series are deduced readily.

### Velocity Profiles

From Eq. (27), the velocity in the boundary layer is simply

$$u=F(f_0'+\xi f_1'+\xi^2 f_2') \tag{37}$$

or

$$u/u_i=f_0'+\xi f_1'+\xi^2 f_2' \tag{38}$$

for $F=u_i$ given in Eq. (1). Figures 4 and 5 show $u/u_i$ vs $z$, respectively, for isothermal and adiabatic walls. One observes that at a given $z$, $u/u_i$ increases with $\xi$. This is because, as shown in Eq. (1), the inviscid velocity $u_i$ relative to the wavefront appears to accelerate in the positive $\xi$ direction. In other words, the fluid is expanding from the high pressure to the lower pressure region and the further the downstream distance is from the wavefront the higher the fluid velocity will attend. As a result, even though the viscosity diffusion in the boundary layer tends to increase the boundary growth the acceleration may suppress some growth of the boundary layer. If the boundary-layer thickness is taken to be approximately $z_\delta=4$ from Figs. 4 and 5, Eqs. (25) and (20) give

$$z_\delta=y_\delta/\sqrt{x+t}=4 \tag{39}$$

Thus at a given instance $t$, the boundary layer thickness $y_\delta$ behind the wavefront may grow like $4\sqrt{x+t}$. The larger the time, the slower the growth of the boundary-layer thickness will be with respect to $x$. In other words, the boundary layer grows rapidly immediately behind the expansion wavefront and flattens out further downstream from the wavefront.

A careful comparison between the profiles shown in Figs. 4 and 5 reveals that at a given $z$ the velocity is slightly higher for the isothermal wall due to heat addition from the wall to the fluid.

### Temperature Profiles

The temperature in the boundary layer is

$$\theta=\frac{1}{\gamma}+\left(G-\frac{1}{\gamma}\right)(g_0+\xi g_1+\xi^2 g_2)$$

or

$$\frac{\theta}{\theta_i}=\left[\frac{1}{\gamma}+\left(G-\frac{1}{\gamma}\right)(g_0+\xi g_1+\xi^2 g_2)\right]\Big/G \tag{40}$$

The solutions are plotted in Fig. 6. The temperature in the boundary layer is seen to be higher than that in the freestream and the value of $\theta/\theta_i$ increases with $\xi$ as a result of an increasing viscous heating in the boundary layer. Figure 6 shows that at $\xi=0.3$ the wall temperature is higher than the local inviscid temperature almost by 10%.

Figure 6 also shows that because of heat addition to the fluid from the wall, the surface temperature for the

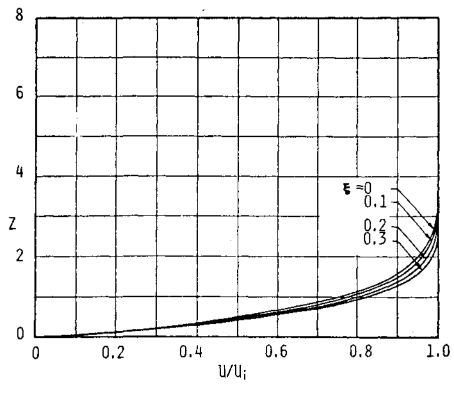


Fig. 4 Velocity profiles for an isothermal wall at $\xi=0$, 0.1, 0.2, and 0.3.

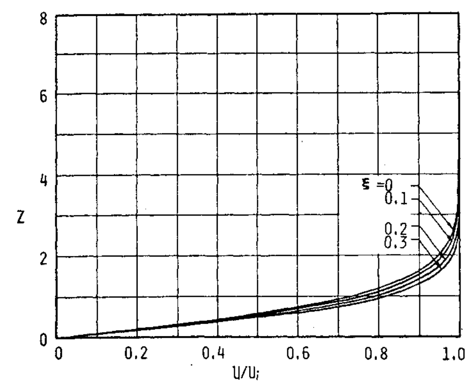


Fig. 5 Velocity profile for an adiabatic wall at $\xi=0$, 0.1, 0.2, and 0.3.

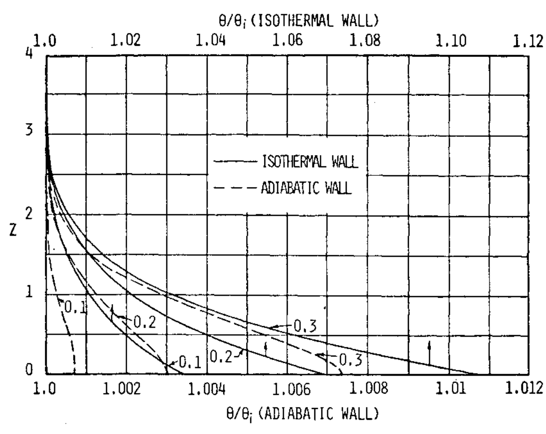


Fig. 6 Temperature profiles at $\xi=0$, 0.1, 0.2, and 0.3.

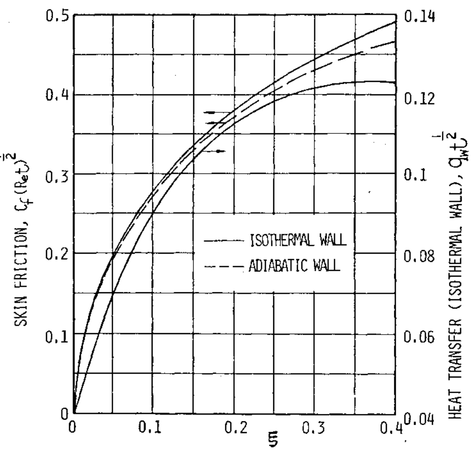


**Fig. 7 Skin friction and heat transfer.**

**Table 3 Skin friction and heat transfer**

| $\xi$ | $C_f\,(Ret)^{1/2}$ Isothermal | Adiabatic | $q_w t^{1/2}$ Isothermal |
|---|---|---|---|
| 0 | 0.0000 | 0.0000 | 0.0000 |
| 0.025 | 0.1469 | 0.1465 | 0.0491 |
| 0.050 | 0.2054 | 0.2042 | 0.0675 |
| 0.075 | 0.2487 | 0.2465 | 0.0803 |
| 0.100 | 0.2839 | 0.2805 | 0.0901 |
| 0.125 | 0.3138 | 0.3091 | 0.0978 |
| 0.150 | 0.3398 | 0.3337 | 0.1041 |
| 0.175 | 0.3627 | 0.3553 | 0.1090 |
| 0.200 | 0.3833 | 0.3743 | 0.1130 |
| 0.225 | 0.4018 | 0.3912 | 0.1161 |
| 0.250 | 0.4185 | 0.4063 | 0.1186 |
| 0.275 | 0.4337 | 0.4199 | 0.1205 |
| 0.300 | 0.4476 | 0.4321 | 0.1218 |
| 0.325 | 0.4603 | 0.4431 | 0.1226 |
| 0.375 | 0.4824 | 0.4618 | 0.1231 |
| 0.400 | 0.4920 | 0.4697 | 0.1228 |
| 0.450 | 0.5087 | 0.4831 | 0.1214 |
| 0.500 | 0.5224 | 0.4939 | 0.1191 |

isothermal wall is higher than that for the adiabatic wall by 3.34% at $\xi = 0.1$, 6.6% at $\xi = 0.2$, and 10.9% at $\xi = 0.3$ giving the temperature ratio $T_w$ (isothermal) to $T_w$ (adiabatic) of approximately $(1 + 0.335\xi)$. Hall considered the case allowing for wall temperature change as occurs with a finite wall thermal conductivity.[6] He found that the temperature in the boundary layer on an adiabatic wall is the same as the temperature in the inviscid freestream. This, in fact, is equivalent to the zero-order solution of Eq. (40), i.e., $\xi = 0$.

### Heat Transfer

For an isothermal wall the local heat transfer from the wall to the fluid is

$$Q_w = -k\frac{\partial T}{\partial Y}\bigg|_{Y=0} \tag{41}$$

Written in dimensionless form, it becomes

$$q_w = -\frac{\partial \theta}{\partial y'}\bigg|_{y'=0} \tag{42}$$

Transformed into $(\xi, z)$ coordinate system, it is

$$q_w = -t^{-1/2}\gamma H\xi^{-1/2}\left(G - \frac{1}{\gamma}\right)[g_0'(0) + \xi g_1'(0) + \xi^2 g_2'(0)] \tag{43}$$

The values of $g_0'$, $g_1'$, and $g_2'$ are, respectively, 0.9575, 0.15074, and $-0.25445$. Figure 7 and Table 3 show that at a given instant the heat transfer increases rapidly behind the wavefront until it approaches a maximum, and then likely decreases. This can be explained as a result of an interplay among the expansion of the freestream, the growing boundary-layer thickness, and the viscous heating. From Eq. (2) we notice that the freestream temperature decreases with the increasing distance from the wavefront. Consequently, heat transfer is from the wall to the fluid. On the other hand, the combined effect of the growing boundary-layer thickness and the viscous heating provides a resistance to the heat transfer further downstream. Equation (43) shows that the heat transfer at a given location decreases with respect to time and is approximately proportionate to $t^{-1/2}$. Physically this is because at a given location the boundary layer grows in time after the expansion wave passes by. The growth of the boundary layer deters the heat transfer.

The coefficient of local heat transfer is determined by Newton's cooling law

$$Q_w = h(T_w - T_i)$$

or

$$h = q_w R(Rek)^{-1/2}[(1/\gamma) - G]^{-1} \tag{44}$$

where $R$ is the gas constant. The function $G$ is given in Eq. (2).

### Skin Friction

The friction coefficient on the wall is defined as

$$C_f = \frac{1}{\rho U_r^2}\bar{\mu}\frac{\partial U}{\partial Y}\bigg|_{Y=0} \tag{45}$$

After coordinate transformation and series expansion, Eq. (45) becomes

$$C_f = (Ret\xi)^{-1/2}FH[f_0''(0) + \xi f_1''(0) + \xi^2 f_2''(0)] \tag{46}$$

The values of $f_0''(0)$, $f_1''(0)$, and $f_2''(0)$ are, respectively, 1.1284, 0.7946, 0.41781 for isothermal wall and 1.1284, 0.65896, 0.32903 for adiabatic wall. The plot of $C_f(Ret)^{1/2}$ is also given in Fig. 7 and Table 3. There is no large difference in skin friction between the isothermal wall and the adiabatic wall for they have very similar velocity profiles as shown in Figs. 4 and 5. Specifically, at $\xi = 0.3$ the skin friction for the isothermal wall is approximately 5.5% higher than that for the adiabatic wall.

## IV. Conclusions

Solutions are obtained for the unsteady compressible laminar boundary-layer flow developed within a centered expansion wave for isothermal and adiabatic walls. The method of similarity transformation via one-parameter groups demonstrates to be a valuable means to the present analysis. The solutions have an accuracy of second-order in $\xi$, which provides an improved solution for the Hall's zero-order solution for the temperature in the boundary layer subject to an adiabatic wall. The present results show that at a given location, the isothermal wall surface temperature is found to be higher than the adiabatic wall surface temperature by a factor of approximately 0.335 $\xi$.

## Appendix

**Function $F^*$ of Eq. (33)**

$$F^*(z) = \left(\frac{3\gamma - 1}{\gamma + 1}\right)f_1''' - \left(\frac{1}{2}\frac{\gamma - 1}{\gamma + 1}\right)zf_1'' - \left(\frac{3}{\gamma + 1}\right)f_0 f_1''$$

$$-\left(\frac{5}{2} + 2\frac{\gamma - 1}{\gamma + 1}\right)f_1' + \left(\frac{6}{\gamma + 1}\right)f_0' f_1' - \left(\frac{5}{\gamma + 1}\right)f_0'' f_1$$

$$
-\frac{3\gamma^2-\gamma}{(\gamma+1)^2}f_0''' + 3\left(\frac{\gamma-1}{(\gamma+1)^2}\right)f_0''f_0 + \frac{3}{2}\frac{\gamma-1}{\gamma+1}f_0'
$$

$$
-2\frac{\gamma-1}{(\gamma+1)^2}f_0'f_0' + 2\frac{\gamma-1}{\gamma+1}g_1 - \left(\frac{\gamma-1}{\gamma+1}\right)^2 g_2
$$

**Function $G^*$ of Eq. (34)**

$$
G^*(z) = \frac{1}{Pr}\left(\frac{1}{2}\frac{\gamma-1}{\gamma+1} + \frac{2\gamma}{\gamma+1}\right)g_1'' + \left(\frac{1}{4}\frac{\gamma-1}{\gamma+1}z\right)g_1'
$$

$$
-\frac{3}{\gamma+1}f_0 g_1' - \left(2 - \frac{\gamma-1}{2(\gamma+1)}\right)g_1 + \frac{4}{\gamma+1}f_0' g_1
$$

$$
-\frac{1}{Pr}\left(\frac{\gamma-1}{(\gamma+1)^2} + \frac{\gamma}{\gamma+1}\right)g_0'' - \frac{5}{\gamma+1}f_1 g_0'
$$

$$
+\left(\frac{3}{2}\frac{\gamma-1}{(\gamma+1)^2}\right)f_0 g_0' - \left(\frac{\gamma-1}{\gamma+1} - \left(\frac{\gamma-1}{\gamma+1}\right)^2\right)g_0
$$

$$
-\frac{4\gamma}{(\gamma+1)^2}f_0''^2 - \frac{2(\gamma-1)}{(\gamma+1)^2}f_0' - \frac{2}{\gamma+1}f_1' + \left(2\frac{\gamma-1}{(\gamma+1)^2}\right)f_0' g_0
$$

$$
+\frac{2}{\gamma+1}f_1' g_0 + \frac{\gamma-1}{\gamma+1} - \left(\frac{\gamma-1}{\gamma+1}\right)^2 - \frac{4}{\gamma+1}f_0'' f_1''
$$

## References


[1] Ludweig, H., "Tube Wind Tunnel: A Special Type of Blowdown Tunnel," AGARD Rept. 143, July 1957.

[2] Riemann, B., "Ueber die Fortpflanzung ebener Luftwellen von endlicher Schwingungsweite," *Abh. der Koniglichen Gessellschaft der Wissenschaften*, Vol. 8, pp. 43-65, 1858-1859.

[3] Huber, P. W., Fitton, C. E., and Delpino, F., "Experimental Investigation of Moving Pressure Disturbance and Shock Waves and Correlation with One-Dimensional Unsteady-Flow Theory," NACA TN 1903, 1949.

[4] Mirels, H., "Boundary Layer behind Shock or Thin Expansion Wave Moving into Stationary Fluid," NACA TN 3712, 1956.

[5] Cohen, N. B., "A Power-Series Solution for the Unsteady Laminar Boundary-Layer Flow in an Expansion Wave of Finite Width Moving Through a Gas Initially at Rest," NACA TN 3943, 1957.

[6] Hall, J. G., "Laminar Boundary Layer Developed within Unsteady Expansion and Compression Waves," *AIAA Journal*, Vol. 10, April 1972, p. 499.

[7] Howarth, L., "Concerning the Effect of Compressibility of Laminar Boundary Layers and Their Separation," *Proceedings of the Royal Society*, Series A, Vol. 194, 1948, p. 16.

[8] Morgan, A.J.A., "The Reduction by One of the Number of Independent Variables in Some System of Partial Differential Equations," *Q. J. M.*, 1952, p. 250.

[9] Hansen, A. G., *Similarity Analyses of Boundary Value Problems in Engineering*, Prentice Hall, Englewood Cliffs, N.J., 1964.

[10] Chang, L. M., "Unsteady Compressible Boundary Layer Flows within a Centered Expansion Wave and Behind a Strong Plane Blast Wave," Ph.D. Dissertation, The University of Iowa, Dec. 1972.